Climatic Change (2025) 178:176
https://doi.org/10.1007/s10584-025-04030-2

Nighttime land surface temperature and thermal discomfort in a seasonally muggy climate

Nkosi Muse[1,2,3] · **Brian D. McNoldy**[4] · **Amy Clement**[4] · **Katharine J. Mach**[2,3]

Received: 3 November 2024 / Accepted: 9 September 2025
© The Author(s) 2025

Abstract
Globally, increasing air moisture can limit not only the human body's ability to cool down, but also that of the Earth's surface. This interaction, however, remains understudied—especially across subtropical-to-tropical regions that experience high levels of humidity. Here, we examine how air moisture influences nighttime land surface temperatures (LSTs), as well as what this interaction means for thermal comfort overnight. During summer months across seasonally muggy Southern Florida, during which time air moisture reaches the highest values of any place in the United States, we examine: 1) how air moisture, measured as specific humidity, varies with urbanicity and geography; 2) whether air moisture limits LST cooling at night; and 3) the implications of increased air moisture and nighttime LSTs for thermal comfort overnight. Based on data from 30 weather stations, we find that nighttime LST remains higher and closer to daytime highs in areas with increased specific humidity, highlighting a decreased surface cooling phenomenon in more humid areas. Both urban and coastal areas exhibit higher nighttime LSTs that are strongly related to thermal discomfort—also resulting in more time spent at or above critical thresholds for thermal discomfort overnight. This analysis therefore underscores the importance of heat mitigation and adaptation strategies that reduce LSTs and anthropogenic heat inputs in seasonally muggy climates in order to increase thermal comfort, especially near coastlines at lower latitudes.

Keywords Land surface temperature · Specific humidity · Thermal comfort · Water vapor

✉ Nkosi Muse
nkosimuse@g.harvard.edu

[1] Center for the Environment, Harvard University, Cambridge, MA 02138, United States of America

[2] Department of Environmental Science and Policy, Rosenstiel School of Marine, Atmospheric, and Earth Science, University of Miami, Miami, FL, United States of America

[3] Leonard and Jayne Abess Center for Ecosystem Science and Policy, University of Miami, Coral Gables, FL, United States of America

[4] Department of Atmospheric Sciences, Rosenstiel School of Marine, Atmospheric, and Earth Science, University of Miami, Miami, FL, United States of America

Published online: 08 October 2025

1 Introduction

Across subtropical-to-tropical regions, heat hazards are exacerbated by the presence of high amounts of air moisture (i.e., water vapor), especially during the warm season (Raymond et al. 2020). Increased air moisture can limit cooling of the human body, reducing thermal comfort and increasing heat stress (Baldwin et al. 2023; Di Napoli et al. 2023; Hanna and Tait 2015; Matthews 2018; Zhang et al. 2023). These thermal environments are typically characterized by "muggy" dew point temperatures, which are frequently used as meteorological proxies for the humidity of the air—that is, the amount of water vapor the air holds. For example, in "seasonally muggy" climates, where average dew point temperatures remain above 65 °F (~18.3 °C) during the warm season, the air is considered to contain what the U.S. National Weather Service has labeled "muggy" to "oppressive" amounts of air moisture, associated with dangers to human health (NOAA n.d.-a).

As compared to more arid climates, regions with seasonally muggy climates can have additional consequences for heat hazards overnight through more limited nighttime cooling (Feng et al. 2020; Hwang 2024; Li et al. 2019; Yin et al. 2020). Effective radiative cooling of land surfaces can be inhibited by an intensified greenhouse effect, where higher concentrations of water vapor absorb and reemit more longwave radiation back to the surface (Chang and Zhang 2019; Dai 2006; Dong et al. 2019; Held and Soden 2000; Hossain and Gu 2016; Liu et al. 2019; Sherwood et al. 2018). Such a phenomenon is significant in areas that exhibit elevated land surface temperatures (LSTs) (e.g., surface urban heat islands) (Athukorala and Murayama 2020; Haashemi et al. 2016; Lemoine-Rodríguez et al. 2022; Manoli et al. 2020; Muse et al. 2022, 2024; Peng et al. 2012; Wu et al. 2019; Zhou et al. 2019) and in coastal areas that are near sources of abundant air moisture (Raymond et al. 2021; Virmani and Weisberg 2005; Yang et al. 2023). In the absence of solar radiation, the surface is a primary source of energy to heat the air of the lower atmosphere (Bechtel 2015; Hulley et al. 2019; Tomlinson et al. 2011). With increased air moisture, elevated nighttime LSTs may, in turn, increase nighttime surface air temperatures (SATs; the ambient temperature that humans experience) and other measures of thermal comfort (e.g., heat index, wet bulb temperature) (Chung et al. 2020; Hulley et al. 2019; NOAA and CDC 2024; Shandas et al. 2019; Yao et al. 2011; Zeng et al. 2015). These factors could also potentially exacerbate daytime heat hazards into the following day (Muse et al. 2024). Such a thermal environment in seasonally muggy climates can be dangerous to human health, as stress on the body is exacerbated by a lack of respite from heat hazards across the diurnal cycle (Di Napoli et al. 2023; He et al. 2022; Raymond et al. 2021; Rogers et al. 2021). These relationships among air moisture, LST, and thermal comfort, however, remain understudied across regions with seasonally muggy climates.

Understanding the relationships among air moisture, LST, and thermal comfort can inform heat response priorities in seasonally muggy climates. If thermal comfort is decreased as a result of higher nighttime LSTs in seasonally muggy climates, reducing surface absorption of daytime solar radiation in ways that ensure that air moisture is not further increased becomes an important consideration for local heat mitigation. Such a consideration would be of increased importance in muggy climates as opposed to drier climates, where a dry atmosphere more freely allows for the reemission of longwave radiation through the lower atmosphere. Potential response options include the expansion of tree canopy cover focused on species with lower evapotranspiration rates (Chàfer et al. 2020; Qiu et al. 2013; Yang et

al. 2023; Zhang and Dai 2022), measures to increase albedo or surface reflectance (Akbari et al. 2001; Priyadarsini et al. 2008; Taha et al. 1988), or cool roofs (Takebayashi and Moriyama 2007; Wang et al. 2022; Zonato et al. 2021). These response options can also improve thermal comfort during the day for outdoor workers and commuters using public transit (e.g., at bus and train stops). In addition, these responses can reduce the need for energy-dependent cooling methods such as air conditioning and thereby decrease energy burdens, emissions, and heat inputs into urban heat islands (UHIs) (Akbari et al. 2001; 'Cathy' Li et al. 2024; Mohammed et al. 2024; Taha et al. 1988; Zhao and Zhang 2023). Further, ensuring that buildings and homes are weatherized in ways that maintain cooler and drier air indoors, as well as limit contributions of excess heat to the lower atmosphere, is also of high priority in seasonally muggy climates, where nighttime outdoor temperatures are a greater hazard (Litardo et al. 2022; NOAA and CDC 2024; Stone and Rodgers 2001; Turek-Hankins et al. 2025; Vijayan et al. 2022; Yurchenko et al. 2019).

Using the case of seasonally muggy Southern Florida, this study seeks to examine the relationships among air moisture, LST, and thermal comfort across summer months (June–August, 2015–2024) when local dew points remain above 22 °C, on average. With data from 30 quality-controlled weather stations, we ask: 1) How does air moisture vary with urbanicity and geography across summertime, tropical Southern Florida? Urbanicity is measured as impervious surface, and geography as latitude and proximity to the coast. 2) Does air moisture limit LST cooling at night? And 3) what are the implications of increased air moisture and nighttime LSTs for thermal comfort at night in this seasonally muggy climate, where thermal comfort is assessed through three commonly used measures: SAT, heat index, and wet bulb temperature. The results of this study provide insight into factors that can exacerbate heat exposures in regions that experience seasonally muggy climates, which can inform appropriate heat mitigation and risk reduction strategies. In addition, this study has important applications for future climate adaptation planning as water vapor concentrations increase under the implications of a warming climate. Seasonally muggy, subtropical-to-tropical regions with increased air moisture may require unique heat responses as compared to more arid or temperate regions.

2 Materials and Methods

2.1 Study area

The Southeastern United States is, on average, the warmest and most humid region of the country (Carter et al. 2018). With an annual mean temperature of 21.5 °C (70.7 °F), Florida is not only the warmest state in the Southeast region but also the warmest across the continental United States (National Oceanic and Atmospheric Administration 2023). The state also experiences the country's highest nighttime, or minimum, temperatures (US Department of Agriculture 2023). While most of the state falls under a humid subtropical classification (Cfa), Southern Florida, the focus area of the study, experiences the most tropical climate across the continental United States during summer months (Köppen-Geiger climate classifications: Aw: tropical savanna, Am: tropical monsoon, and Af: tropical rainforest) (Beck et al. 2023; Kottek et al. 2006) (Fig. S1). Florida's unique geography along the peninsula greatly influences the state's climate and weather conditions (Cloutier-Bisbee et

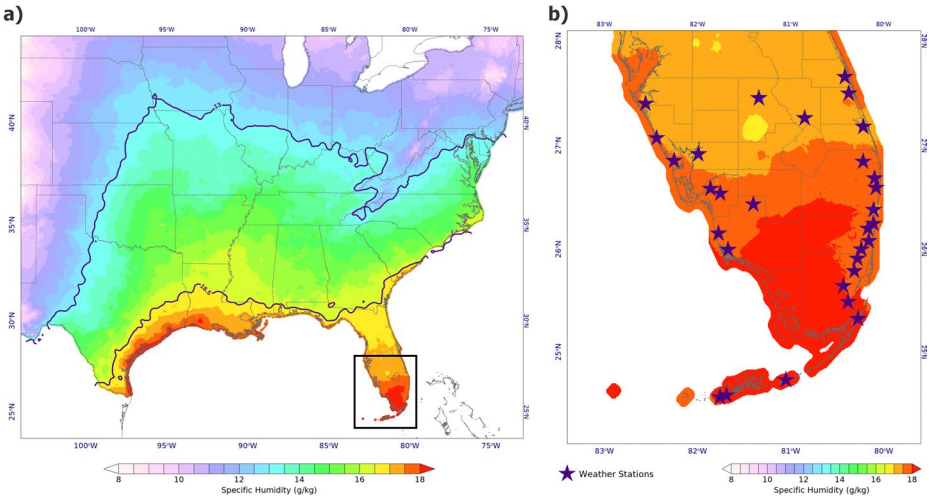


Fig. 1 Mean summer (June–August, 1991–2020) specific humidity (g/kg) across the eastern United States (**a**) and seasonally muggy Southern Florida, the area of study (**b**). (**a**) The northern contour line highlights the 13 g/kg threshold for mean summer specific humidity, while the southern contour line highlights the 16.5 g/kg threshold; these are approximately equivalent to dew point temperatures of 18 and 22 °C (65 and 72 °F). The black box highlights the area of study. (**b**) Stars indicate the 30 weather stations used for analysis across Southern Florida

al. 2019; Winsberg 2011). The Gulf of Mexico to the west and the Atlantic Ocean to the east maintain the U.S.'s highest levels of air moisture across the state, especially during summer months (Fig. 1) (Zierden and Griffin 2014).

2.2 Data

LST data from the Moderate Resolution Imaging Spectroradiometer (MODIS) instrument were retrieved from the NASA Terra satellite. The MODIS instrument orbits Earth at 1-to-2-day cycles, capturing LST data at 1-kilometer resolution within 36 spectral bands (National Aeronautics and Space Administration 2023). More specifically, MOD11A2 Version 6 data were used, where each 1-kilometer pixel represents an average 8-day LST value in Kelvin (Wan et al. 2015). Although other satellites such as Landsat and ECOSTRESS capture LST data at higher resolution, MODIS captures both daytime and nighttime LST most consistently and with the highest spatial coverage. MODIS data are cloud masked before download from the USGS EarthExplorer website (USGS 2023), and the 8-day average LST provides the best surface coverage with reduced cloud interference. The Florida peninsula falls within horizontal tile 10 and vertical tile 6 of the Terra satellite's record database. 119 scenes were downloaded and utilized for this study.

Automated Surface Observing System (ASOS) network weather station data were retrieved from the Iowa Environmental Mesonet (Iowa State University 2023) for 30 Southern Florida weather stations (Fig. 1; Table S1). Daily SAT and parameters for the calculation of specific humidity and other thermal comfort indices were downloaded for summer (June–August) 2015–2024 at hourly intervals for each weather station.

Available impervious surface data for 2017, 2019, 2021, and 2023 were downloaded from the National Land Cover Database (NLCD) at 30-meter resolution (National Land

Cover Database 2023). Each 30x30m pixel value represents a percentage of impervious surface (0–100%) for that area.

2.3 Methodology

This study used airport weather station data and MODIS satellite imagery to examine the role of air moisture for nighttime cooling across the seasonally muggy Florida peninsula during summer months (June–August, 2015–2024). LST data, processed in ArcGIS Pro software (Environmental Systems Research Institute (ESRI) 2021), were converted to Celsius (°C) with a scale factor of 0.02. Statistical analyses were performed to explore modulating factors for specific humidity, nighttime LST, and diurnal LST (defined as the difference between daytime and nighttime LST) across the study region. Nighttime and diurnal LSTs were then examined to understand the roles that air moisture and geographical factors (urbanicity, latitude, proximity to coast) play in potentially limiting surface cooling overnight. The relationships between nighttime and diurnal LST and thermal comfort indices (SAT, heat index, wet bulb temperature) were also explored. All statistical analyses were performed in R (Posit team 2024).

2.3.1 Specific Humidity

Specific humidity (q) is the mass of water vapor per mass of moist air (American Meteorological Society 2022). As opposed to dew point temperature (°C), the amount of moisture in the air is quantified as specific humidity (g/kg)—the ratio of the mass of water vapor to the mass of moist air. Specific humidity in Fig. 1 was calculated from Parameter-elevation Regressions on Independent Slopes Model (PRISM) Climate Group dew point data at 800-meter resolution using elevation and barometric pressure (European Centre for Medium-Range Weather Forecasts (ECMWF) n.d.; National Science Foundation and MetPy n.d.; PRISM Climate Group 2023). For airport station data analysis, specific humidity was calculated utilizing equations from Bolton (1980):

$$e = 6.112(\exp(\frac{17.67 * T_d}{T_d + 243.5})),$$

where e represents vapor pressure in millibars, and T_d represents the dew point temperature (°C). With e, q can be calculated in g/kg:

$$q = \frac{(0.622 * e)}{(p - (0.378 * e))} \times 1000,$$

where p represents the surface pressure in millibars. Limitations for using Bolton's equation to determine specific humidity (i.e., temperatures outside −35 °C to 35 °C) did not apply to this study's analysis.

2.3.2 Wet bulb temperature

Wet bulb temperature (T_w) (closely related to Wet Bulb Globe Temperature (National Oceanic and Atmospheric Administration n.d.) represents the lowest possible temperature to which the SAT (also known as dry bulb temperature) can be cooled via evaporation (National Wildfire Coordinating Group n.d.) Such a measure is important because it can indicate how much the human body is able to cool down via the evaporative cooling of sweat. At 100% relative humidity, the wet bulb temperature is equal to the SAT, as the air cannot be cooled further via evaporation due to saturation. Wet bulb temperature (°C) was estimated using an equation from Stull (2011):

$$T_w = T\tan^{-1}(0.151977\sqrt{RH + 8.313659}) + \tan^{-1}(T + RH) - \tan^{-1}(RH - 1.676331) + 0.00391838\sqrt{RH}^{3}\tan^{-1}(0.023101 \times RH) - 4.686035,$$

where T represents SAT (°C) and RH represents relative humidity (%).

2.3.3 Statistical analysis

Multiple linear regression was performed to examine the relationships that specific humidity, nighttime LST, and diurnal LST share with relevant predictor variables across Southern Florida. Predictor variables included proximity to the coast (kilometers), impervious surface (%), latitude (for specific humidity), and daytime LST (°C). Average specific humidity was calculated at each station (2015–2024) from daily observations. Impervious surface represents the mean value of pixels (% impervious surface) aggregated within a 1-kilometer (km) buffer around a weather station. Variance inflation factors (VIFs), key metrics of multicollinearity or a predictor variable's level of correlation with other predictor variables in a multiple regression model, were calculated to ensure the quality of analysis (Murray et al. 2012). High VIF values (VIF >5) indicate inflation of the variance of a variable's coefficient, potentially resulting in a misrepresentation of the predictor variable's impact on the dependent variable.

Average nighttime (12 AM local time) specific humidity values (June–August, 2015–2024) were compared to mean nighttime LST (12 AM) values measured at each station. Mean daytime and nighttime LST pixels were calculated for 2015–2024 across Southern Florida. Mean LST pixels were then aggregated to their mean value within a weather station's 1-km buffer for analysis with specific humidity and predictor variables. Diurnal LST was calculated by subtracting mean nighttime LST pixels from daytime LST pixels within weather station 1-km buffers. Pearson's correlation was used for comparative analysis.

To understand the role that nighttime LST plays in nighttime thermal comfort, nighttime LST was compared to nighttime SAT, heat index, and wet bulb temperature at each station. Since MODIS nighttime imagery is captured at 12 AM, nighttime LST was compared to 12 AM SAT, heat index, and wet bulb temperature observations. The relationships between thermal comfort and factors that contribute to increased specific humidity and LSTs were also examined, with implications for understanding where nighttime thermal stress may be most elevated.

3 Results

3.1 Modulating factors for specific humidity

In Southern Florida, specific humidity increases with decreasing latitude and increased proximity to the coast, as expected. Although this trend is not obvious to the eye in Fig. 2a, especially north of the Florida Keys, multiple regression analysis shows latitude (−0.344) and proximity to coast (−0.41) as statistically significant predictor variables for air moisture across the study region (Table S2). Also shown as statistically significant in the multiple regression model for specific humidity is the interaction between geographical factors, latitude, and proximity to the coast, where specific humidity increases with simultaneous decreasing latitude and distance to the coast. The four weather stations located in the Florida Keys (EYW, K70, MTH, NQX) are a key example of this interaction effect, as Florida Keys stations are located at an average latitude of 24.79 °N and sit at an average proximity to the coast of 0.76 km. Together, the archipelagic geography and low latitude of the Florida Keys result in the highest specific humidity observations of the study region, with an average value of 18.8 g/kg across the study period (2015-2024). For context, specific humidity's

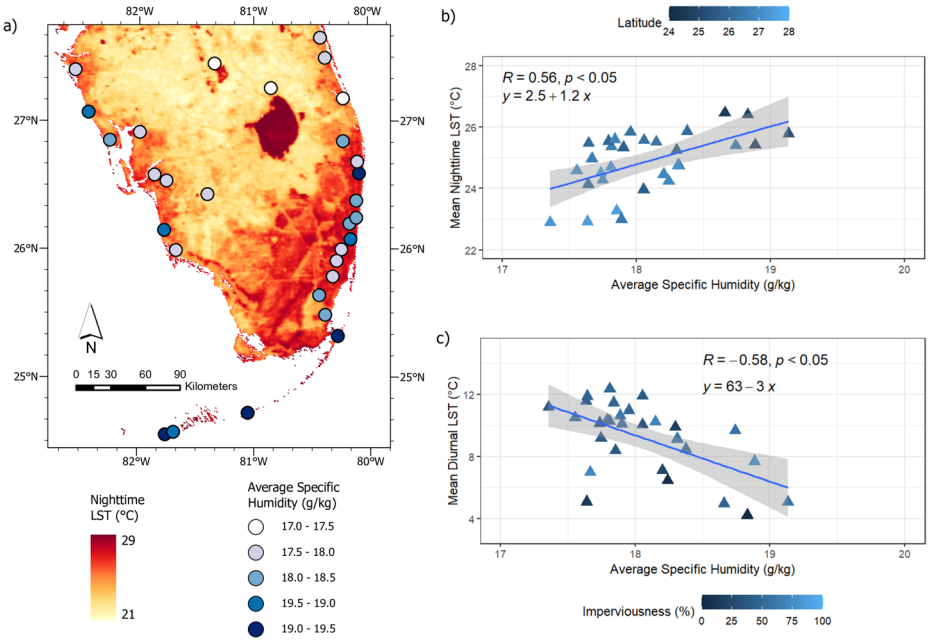


Fig. 2 Nighttime LST and specific humidity across Southern Florida, as well as specific humidity's relationship with nighttime and diurnal LST. (**a**) Each circle represents the average daily summer (June–August, 2015–2024) specific humidity observed at each station. Each 1-km LST pixel represents the mean nighttime (12 AM) LST value for that location over the study period. (**b**) Each data point represents an average summer-specific humidity value observed at each weather station versus the mean summer nighttime LST value within a 1-km buffer around the corresponding weather station, colored by latitude. (**c**) Each data point represents an average summer-specific humidity value observed at each weather station versus the mean summer diurnal LST value within a 1-km buffer around the corresponding weather station, colored by mean impervious surface (%). Grey shading around the regression lines indicates a 95% confidence interval

daily average (June–August, 2015–2024) across all weather stations (n = 30) is 18.1 g/kg. Urbanicity, the third predictor variable for air moisture used in the analysis, was statistically insignificant in the multiple regression model (Table S2, S3).

3.2 Nighttime and diurnal LST

Across the study region, nighttime LSTs remain higher where air moisture concentrations are increased, at a rate of 1.2 °C per unit (g/kg) increase of specific humidity (Fig. 2b). This finding was supported by multiple regression analysis, with other predictor variables (proximity to coast and imperviousness) held constant (Table 1). Proximity to the coast is also a statistically significant predictor variable for nighttime LST, where nighttime LST is predicted to decrease by 0.02 °C per kilometer of distance away from the coast. Surprisingly, there was also no significant relationship found between nighttime LST and imperviousness. Although urban nighttime LSTs are generally higher in more urban areas, mean nighttime LSTs in more rural areas remain within 1 °C of urban nighttime LSTs (Table S3). Daytime LST, a measure typically highly and positively correlated with imperviousness, also exhibits a positive relationship with nighttime LST (Table 1). For every 1 °C increase in daytime LST, we can expect nighttime LST to increase (or remain higher) by 0.18 °C. Such a finding is not surprising, as the warmth of the surface during the daytime can play a significant role in how warm the surface remains at night. Like specific humidity, nighttime LST is also highest on average (26.0 °C) across Florida Keys weather stations (24.9 °C across all weather stations).

Like nighttime LST, the differences between daytime and nighttime LSTs (diurnal LSTs) exhibit a statistically significant relationship with specific humidity across the study region, as diurnal LSTs are smaller where specific humidity is increased. Fig. 2c displays the relationship between diurnal LST and specific humidity across the 30 weather stations, where differences in daytime and nighttime LST decrease by 3 °C per unit increase in air moisture (g/kg). Multiple regression analysis supports this correlation. When holding latitude, imperviousness, and coastal proximity constant, diurnal LST decreases by 2.798 °C per g/kg increase in specific humidity (Table 2). Impervious surface has an opposite, statistically significant effect on differences in daytime and nighttime LST (0.04 °C increase per percent

Table 1 Southern Florida nighttime LST (°C) vs predictor variables. The relationships between nighttime LST and average specific humidity, proximity to coast, mean daytime LST, and mean imperviousness are provided, as measured at weather stations (n = 30). Each coefficient can be interpreted as a change in nighttime LST (°C) per a unit change in a variable, while other variables are held constant (e.g., one kilometer increase in distance to the coast equals a 0.022 decrease in nighttime LST (°C))

Independent Variable	Coefficient	Std. Error	p-value	VIF
Average Specific Humidity (g/kg)*	1.111	0.313	$p = 0.002$	1.439
Proximity to coast (km)*	−0.022	0.006	$p = 0.002$	1.239
Mean Daytime LST (°C)*	0.175	0.060	$p = 0.007$	1.381
Mean Impervious Surface (%)	−0.000	0.007	$p = 0.986$	1.222
				*Statistically significant ($p \leq 0.05$)
		Constant	**Adjusted R-Squared**	**Model *p*-value**
		−0.895	0.60	$p = 0.000$

Table 2 Southern Florida difference in mean daytime and nighttime (diurnal) LST (°C) vs predictor variables. The relationships between diurnal LST and average daily specific humidity, mean imperviousness, and proximity to coast are provided, as measured at weather stations ($n = 30$). Each coefficient can be interpreted as a unit change in diurnal LST per a unit increase in a variable, while other variables are held constant (e.g., one percent increase in mean imperviousness equals a 0.039 °C increase in diurnal LST)

Independent Variable	Coefficient	Std. Error	*p*-value	VIF
Average Specific Humidity (g/kg)*	−2.798	0.82	$p = 0.002$	1.219
Mean Impervious Surface (%)*	0.039	0.018	$p = 0.035$	1.007
Proximity to coast (km)	0.012	0.018	$p = 0.513$	1.222
				*Statistically significant ($p \leq 0.05$)
		Constant	**Adjusted R-Squared**	**Model p-value**
		57.88	0.38	$p = 0.001$

increase in mean imperviousness), signifying a wider range of diurnal LST in more urban areas.

3.3 Implications for thermal comfort

Thermal comfort, as measured by SAT, heat index, and wet bulb temperature, decreases across Southern Florida weather stations with increasing proximity to the coast (Fig. 3a, b, c). This finding is similar to nighttime LST, which exhibits a negative relationship with proximity to coast across the study region (Table 1). Heat index values across weather stations increase at the greatest rate per kilometer decrease in distance to the coast (0.06) (Fig. 3b). 93% of weather stations within 25 kilometers of the Southern Florida coast exhibit average nighttime heat index values of "caution" (27 °C, as defined by the National Weather Service (NOAA n.d.-b) or greater, on average.

Nighttime LST is also strongly correlated with thermal discomfort (Fig. 3d, e, f). As expected, where nighttime LSTs are increased, SAT (coefficient = 1.1), heat index (coefficient = 2.2), and wet bulb temperature (0.47) are also increased. Like nighttime LST, these thermal comfort indices also remain higher overnight in more urbanized settings (Table S3). These findings support much of the literature concerning UHIs that are characterized by increased temperatures and thermal discomfort as compared to more rural areas. Nighttime LSTs that are positively influenced by specific humidity account for a significant amount of variance in relationships with thermal comfort ($R > .80$, for all three indices) (Fig. 3d, e, f).

Although only 4 stations have a mean heat index of "extreme caution" (at or above 90 °F or 32.2 °C) as deemed by the local National Weather Service (Miami-Ft. Lauderdale-West Palm Beach) (Fig. 3), all stations reach this threshold throughout the study period (Fig. 4). Figure 4a shows the average number of hours that each station spends at or above a heat index value of "extreme caution" across Southern Florida. Unsurprisingly, Florida Keys stations spend the most amount of time at or above the 90 °F threshold—at least 5.5 hours per summer night (Fig. 4a). Stations with higher amounts of impervious surface are also associated with increased hours at or above "extreme caution" (Table S3). Many of these stations with increased urbanicity are located in Southeast Florida, the state's most urbanized and populous area (US Census Bureau 2025). In addition, Table S3 shows decreased distance to the coast resulting in a greater amount of hours at or above "extreme caution". Lastly,

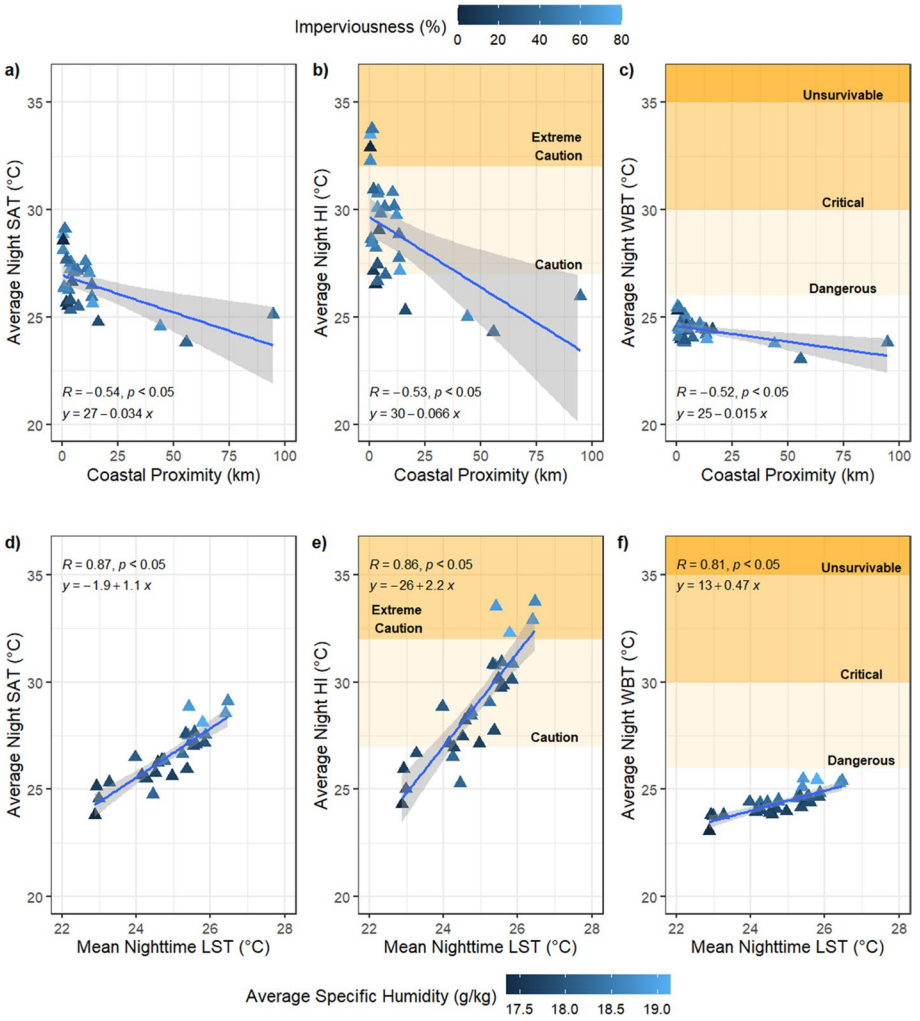


Fig. 3 Nighttime SAT (**a**, **d**), heat index (**b**, **e**), and wet bulb temperature (**c**, **f**) vs coastal proximity and nighttime LST (°C) across Southern Florida weather stations (n = 30). Each triangle represents the average nighttime thermal comfort measure (12 AM) measured at each weather station versus that station's distance to the coast (a, b, c; colored by impervious surface (%)) and the mean of mean summer (June–August, 2015–2024) nighttime (12 AM) LST values within a 1-kilometer buffer around each weather station (d, e, f; colored by average daily specific humidity (g/kg)). Background colors represent "caution" and "extreme caution" heat index thresholds (**b**) as defined by the National Weather Service (NOAA n.d.-b) and "critical" wet bulb temperature thresholds (**c**) as defined across the literature (Raymond et al. 2020; Sherwood and Huber 2010; Vecellio et al. 2022). Grey shading around the regression lines indicates a 95% confidence interval

increased nighttime LST, which also increases with decreased distance to the coast, also has a positive relationship with hours spent at or above the "extreme caution" threshold—a 1.6 hour increase in time spent at or above "extreme caution" per each degree Celsius increase in nighttime LST (Fig. 4b). On the western coast of Southern Florida, weather stations do not spend more than 4 hours above "extreme caution" per night, on average. Despite this,

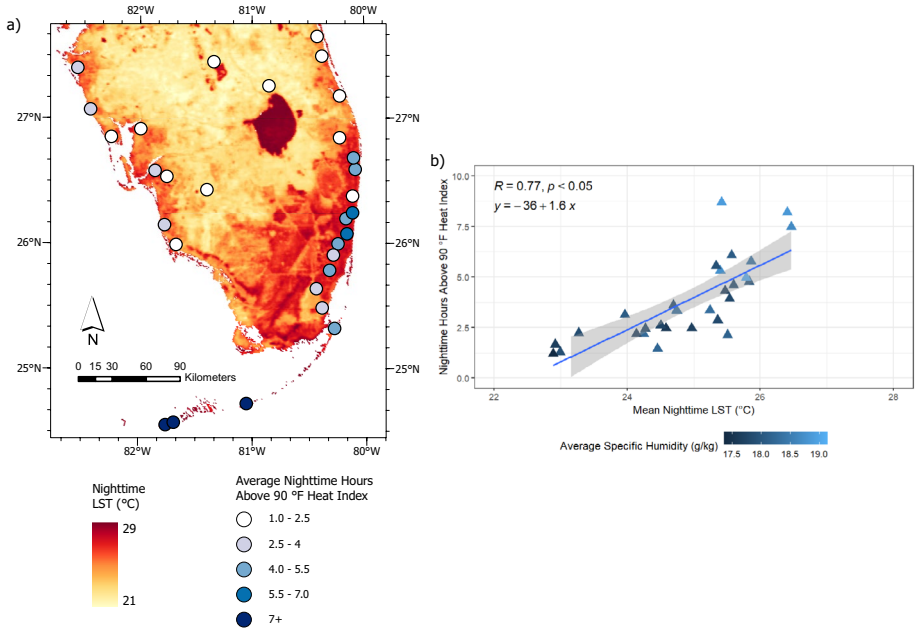


Fig. 4 Nighttime LST and average nighttime hours above an "extreme caution" heat index value (32.2 °C or 90 °F) across Southern Florida. (**a**) Each circle represents the average summer (June–August, 2015–2024) nighttime hours that a station observes a heat index above 90 °F, deemed "extreme caution" by the local National Weather Service. Each 1-km LST pixel represents the mean nighttime (12 AM) LST value for that location over the study period. (**b**) Each triangle represents a weather station's average number of nighttime hours spent above 90 °F versus the mean nighttime LST (°C) within a 1-km buffer around the corresponding weather station, colored by average specific humidity (g/kg). Grey shading around the regression line indicates a 95% confidence interval

all stations remain at "caution" (80.6 °F or 27 °C) on average throughout summer nights across the study period.

4 Discussion

Higher levels of air moisture exacerbate heat hazards, especially in regions that experience "seasonally muggy" climates. In this study, we examine the role that air moisture, as represented by specific humidity, and each of its modulating factors play in influencing nighttime LST and thermal comfort across a seasonally muggy region, as very few studies have done. Specific humidity, which is generally variable across the study region, exhibits a strong, positive relationship with nighttime LSTs. Diurnal LSTs (differences between daytime and nighttime LSTs) also exhibit a statistically significant relationship with air moisture, decreasing with increasing specific humidity. Where nighttime LSTs are higher, thermal discomfort is also decreased, as expected. This is especially true closer to the coast and in more urban regions, where there is an increased average number of nighttime hours at or above heat index values considered to be of "extreme caution". Air moisture's role in

decreasing thermal comfort during the evening hours could intensify under the implications of global warming and requires place-specific responses to ensure human health.

In a peninsular region at lower latitudes, intense solar radiation heats the surface, in turn increasing LSTs during the daytime, but also inducing higher rates of evaporation (Becker and Boyd 1957; Bhatia 2014; Muse et al. 2024; NASA n.d.; Roca et al. 2010) from surrounding waters such as the Gulf of Mexico and the Atlantic Ocean. Nighttime LST can be considered a function of not only daytime heating that is most intense at lower latitudes, but also specific humidity, observed to be higher closer to the coast (Table S2, S3). Coastlines are typically defined by an advection of abundant moisture inland due to the onshore-offshore gradient in temperature (Estoque 1962; Pielke 1973). Such a phenomenon would result in an increased amount of air moisture in coastal areas and subsequently an intensified local greenhouse effect that can limit cooling of the surface, as observed in this study (Chang and Zhang 2019; Dai 2006; Dong et al. 2019; Held and Soden 2000; Hossain and Gu 2016; Liu et al. 2019; Sherwood et al. 2018).

A potential localized greenhouse effect of water vapor in the lower atmosphere was also observed with diurnal LST, as the range between daytime and nighttime LSTs decreases with increasing air moisture (Fig. 2, Table 2). With solar radiation absent, nighttime LSTs that remain higher and closer to their daytime highs can continue to heat the air and contribute to decreased thermal comfort for longer periods of time. This is especially true of stations closer to the coast (Fig. 4), such as in the Florida Keys, where diurnal LSTs of less than 5 °C were observed, with corresponding diurnal heat indices as low as 4 °C. These findings support assumptions made in thermal comfort tools such as the National Weather Service's "HeatRisk" tool, where: 1) more humid air typically leads to warmer overnight temperatures, and 2) smaller differences in daytime highs and overnight lows tend to occur in more humid locations (NOAA and CDC 2024). We hypothesize that similar patterns that can threaten human health across the diurnal cycle also exist along much of the United States' Gulf Coast, which exhibits muggy conditions for much of the year (Greene et al. 2011; Läderach and Raible 2013; Petkova et al. 2015), and even more so in Caribbean islands that are surrounded by warmer bodies of water (Di Napoli et al. 2023). These findings contrast with the effects that increase thermal comfort, such as Chicago's lake effect (Chakraborty et al. 2023) and dynamics along California's Pacific Coast (Gershunov and Guirguis 2012), where cooler waters persist and still allow for land-water breezes that can serve as natural cooling mechanisms. Increased urbanization along the coast, prevalent along Florida coasts, has also been found to be a major factor in weakening land-sea breezes that moderate thermal stress (Shen et al. 2019; Xiao et al. 2023). This coastal urbanization has been linked to decreased ventilation in urban areas, allowing for warmer, more stagnant air masses during the evening hours (Tysa et al. 2019; Yang et al. 2019).

Nighttime LST's positive relationship with specific humidity (Table 1, Fig. 2) can play a key role in decreased thermal comfort (Fig. 3a, b, c). For example, nighttime SAT exhibits a strong, positive relationship with nighttime LST ($R = 0.87$), contrasting relationships found during the day in seasonally muggy climates (Muse et al. 2024). Among nighttime LST and thermal comfort index interactions, the positive relationship between LST and SAT is especially important for multiple reasons: 1) at nighttime, LST is one of the main sources of energy to increase SAT; 2) SAT is a key component of commonly used measures of thermal comfort; and 3) as SAT increases, the capacity of the air to hold additional moisture also increases (Trenberth et al. 2003; Vecellio et al. 2022). Thus, the heat index and wet bulb

temperature, two measures of thermal comfort dependent on SAT and air moisture, are also likely to increase with higher nighttime LSTs (Fig. 4). This is especially true in urban regions that exhibit UHI effects and coastal regions that are near abundant sources of air moisture (Table S3). In seasonally muggy climates, coastal regions that experience increased thermal discomfort as a result of increased urbanization and weakened natural cooling mechanisms (i.e., sea and land breezes) must prioritize heat adaptation solutions in urban planning. For outdoor urban heat hazards, especially those exacerbated by increased absorption of solar radiation by impervious and blackbody surfaces, tree canopy and shading are available solutions (Chen et al. 2020; Jiang et al. 2025; Muse et al. 2024). Indoors, air conditioning is a primary source of relief, especially in moist climates where other complications can arise (e.g., mold and mildew). However, efficiency in building energy attenuation and use is an important factor, as heat from buildings can contribute to increased heat hazards outdoors ('Cathy' Li et al. 2024). Cool and green roofs, as well as solar panels, have also been found to be effective solutions (Jiang et al. 2025; Masson et al. 2014).

This research was not conducted without limitations. First, specific humidity, as well as other parameters and thermal comfort measures observed at weather stations, remain highly hyperlocal (Clement et al. 2023). As such, conditions close to and in between weather stations may vary. A limited availability of weather stations, including inland stations, affected this analysis (60% of stations are located within 5 km of the coast). Additional inland stations can help to identify gradients that may exist in air moisture from inland to coastal stations (Schmitt and Clement 2025; Winsberg 2011), as well as how such a gradient may affect LST and thermal comfort, especially in a region characterized by abundant wetlands (e.g., the Everglades) (US EPA 2024). Second, higher resolution LST data are static and captured at the same time each night. More frequent LST observations at different times of night (or day) for analysis with weather station data could better highlight relationships between specific humidity and LST. Due to cloud cover and other satellite obstructions of the surface, daily observations are also limited.

Future work could also address the role of other greenhouse gases of various potency (e.g., carbon dioxide, CO_2; methane, CH_4; nitrous oxide, N_2O) in limiting surface cooling, with or without the impact of increased water vapor. Such analysis could be especially relevant in urban areas, where anthropogenic heating is at its peak. In addition, many thresholds for thermal comfort are defined by daytime highs in temperature, yet thresholds for thermal comfort during the evening may be different, as physiological impacts of heat hazards and decreased thermoregulation can be different at night. Establishing thresholds for nighttime thermal comfort, both indoors and outdoors, could highlight the differences between daytime and nighttime heat risks.

5 Conclusions

The results of this study highlight the effect of air moisture concentrations on nighttime and diurnal LST across a seasonally muggy region, as well as the consequences for thermal comfort. Nighttime LST remains higher and closer to daytime highs during summertime evening hours in places that have higher specific humidity, highlighting the localized role of water vapor's greenhouse effect. In seasonally muggy regions, adaptation to reduce the risk associated with intensified nighttime and diurnal heat hazards is important, especially in

highly populous urban regions near the coast. Anthropogenic activities such as urbanization have resulted in excess energy being contributed to local energy balances through higher rates of solar radiation absorption and building energy output, increasing local temperatures. In coastal regions at low latitudes where warmer bodies of water result in decreased natural cooling (i.e., land-water breezes, air moisture sources), heat responses that reduce localized energy inputs (e.g., increasing albedo and shading canopy), especially in UHIs, would in turn improve thermal comfort considerations overnight. In addition to these adaptation measures, weatherizing buildings and homes is also of high priority for heat health implications and energy security, as air moisture continues to increase alongside average temperature for the foreseeable future.

Supplementary Information The online version contains supplementary material available at https://doi.org/10.1007/s10584-025-04030-2.

Author contributions **Conceptualization:** Nkosi Muse, Brian D. McNoldy, Amy Clement, Katharine J. Mach; **Methodology:** Nkosi Muse, Brian D. McNoldy, Amy Clement, Katharine J. Mach; **Formal analysis and investigation:** Nkosi Muse; **Writing - original draft preparation:** Nkosi Muse; **Writing - review and editing:** Brian D. McNoldy, Amy Clement, Katharine J. Mach; **Supervision:** Katharine J. Mach

Funding This research was funded by the McKnight Doctoral Fellowship Program of the Florida Education Fund; the Rosenstiel School of Marine, Atmospheric, and Earth Science at the University of Miami; and the University of Miami Laboratory for Integrative Knowledge (U-LINK). A.C. and K.J.M. acknowledge support from the National Science Foundation (award number 2437955). The funders had no role in study design, data collection and analysis, decision to publish, or preparation of the manuscript.

Data availability MODIS land surface temperature data can be downloaded through NASA/USGS EarthExplorer (USGS 2023). Weather station data can be downloaded through the ISU Iowa Environmental Mesonet (Iowa State University 2023). Data processing and analysis and figure production (with the exception of Fig. 1) were performed in ArcGIS Pro Software and R (Environmental Systems Research Institute (Esri) 2021; Posit team 2024). Plots in R were produced using ggplot (Wickham 2016). Fig. 1 was generated in IDL (NV5 Geospatial Software) with data from PRISM (NV5 Geospatial Software NV5 n.d.; PRISM Climate Group 2023).

Declarations

Conflict of interest The authors have no competing interests to declare that are relevant to the content of this article.

Open Access This article is licensed under a Creative Commons Attribution 4.0 International License, which permits use, sharing, adaptation, distribution and reproduction in any medium or format, as long as you give appropriate credit to the original author(s) and the source, provide a link to the Creative Commons licence, and indicate if changes were made. The images or other third party material in this article are included in the article's Creative Commons licence, unless indicated otherwise in a credit line to the material. If material is not included in the article's Creative Commons licence and your intended use is not permitted by statutory regulation or exceeds the permitted use, you will need to obtain permission directly from the copyright holder. To view a copy of this licence, visit http://creativecommons.org/licenses/by/4.0/.

References

Akbari H, Pomerantz M, Taha H (2001) Cool surfaces and shade trees to reduce energy use and improve air quality in urban areas. Solar Energy 70(3):295–310. https://doi.org/10.1016/S0038-092X(00)00089-X

American Meteorological Society (2022) Glossary of meteorology. Specific Humidity. Retrieved December 14, 2023, from https://glossary.ametsoc.org/wiki/Specific_humidity

Athukorala D, Murayama Y (2020) Spatial variation of land use/cover composition and impact on surface urban heat island in a tropical sub-saharan city of Accra, Ghana. Sustainability 12(19):19. https://doi.org/10.3390/su12197953

Baldwin JW, Benmarhnia T, Ebi KL, Jay O, Lutsko NJ, Vanos JK (2023) Humidity's role in heat-related health outcomes: a heated debate. Environ Health Perspect 131(5):055001. https://doi.org/10.1289/EHP11807

Bechtel B (2015) A new global climatology of annual land surface temperature. Remote Sens 7(3):Article 3. https://doi.org/10.3390/rs70302850

Becker CF, Boyd JS (1957) Solar radiation availability on surfaces in the United States as affected by season, orientation, latitude, altitude and cloudiness. Solar Energy 1(1):13–21. https://doi.org/10.1016/0038-092X(57)90050-6

Beck HE, McVicar TR, Vergopolan N, Berg A, Lutsko NJ, Dufour A, Zeng Z, Jiang X, van Dijk AIJM, Miralles DG (2023) High-resolution (1 km) Köppen-Geiger maps for 1901–2099 based on constrained CMIP6 projections. Sci Data 10(1):724. https://doi.org/10.1038/s41597-023-02549-6

Bhatia SC (2014) 2—Solar radiations. In: Bhatia SC (ed) Advanced renewable energy systems. Woodhead Publishing India, pp 32–67. https://doi.org/10.1016/B978-1-78242-269-3.50002-4

Bolton D (1980) The computation of equivalent potential temperature. Monthly Weather Review 108(7):1046–1053. https://doi.org/10.1175/1520-0493(1980)108/3c1046:TCOEPT/3e2.0.CO;2

Carter LM, Terando A, Dow K, Hiers K, Kunkel KE, Lascurain A, Marcy DC, Osland MJ, Schramm PJ (2018) Chapter 19: Southeast. Impacts, risks, and adaptation in the United States: The Fourth National Climate Assessment, Volume II. U.S. Global Change Research Program. https://doi.org/10.7930/NCA4.2018.CH19

Chakraborty Tc., Wang J, Qian Y, Pringle W, Yang Z, Xue P (2023) Urban versus lake impacts on heat stress and its disparities in a shoreline city. Geohealth 7(11):e2023GH000869. https://doi.org/10.1029/2023GH000869

Chang K, Zhang Q (2019) Modeling of downward longwave radiation and radiative cooling potential in China. J Renewable Sustainable Energy 11:066501. https://doi.org/10.1063/1.5117319

Chen J, Jin S, Du P (2020) Roles of horizontal and vertical tree canopy structure in mitigating daytime and nighttime urban heat island effects. Int J Appl Earth Obs Geoinf 89:102060. https://doi.org/10.1016/j.jag.2020.102060

Chàfer M, Pisello AL, Piselli C, Cabeza LF (2020) Greenery system for cooling down outdoor spaces: results of an experimental study. Sustainability 12(15):Article 15. https://doi.org/10.3390/su12155888

Chung J, Lee Y-G, Jang W, Lee S, Kim S (2020) Correlation analysis between air temperature and MODIS land surface temperature and prediction of air temperature using TensorFlow long short-term memory for the period of occurrence of cold and heat waves. Remote Sens 12(19):3231. https://doi.org/10.3390/rs12193231

Clement A, Troxler T, Keefe O, Arcodia M, Cruz M, Hernandez A, Moanga D, Adefris Z, Brown N, Jacobson S (2023) Hyperlocal observations reveal persistent extreme urban heat in southeast Florida. J Appl Meteorol Climatol. https://doi.org/10.1175/JAMC-D-22-0165.1

Cloutier-Bisbee SR, Raghavendra A, Milrad SM (2019) Heat waves in Florida: climatology, trends, and related precipitation events. J Appl Meteorol Climatol 58(3):447–466. https://doi.org/10.1175/JAMC-D-18-0165.1

Dai A (2006) Recent climatology, variability, and trends in global surface humidity. J Climate. https://doi.org/10.1175/JCLI3816.1

Di Napoli C, Allen T, Méndez-Lázaro PA, Pappenberger F (2023) Heat stress in the Caribbean: climatology, drivers, and trends of human biometeorology indices. Int J Climatol 43(1):405–425. https://doi.org/10.1002/joc.7774

Dong M, Chen N, Zhao X, Fan S, Chen Z (2019) Nighttime radiative cooling in hot and humid climates. Opt Express 27(22):31587–31598. https://doi.org/10.1364/OE.27.031587

Environmental Systems Research Institute (ESRI) (2021) ArcGIS Pro (Version 2.9.2) [Computer software]. Retrieved August 28, 2024, from https://www.esri.com/en-us/arcgis/products/arcgis-pro/overview

Estoque MA (1962) The sea breeze as a function of the prevailing synoptic situation. J Atmos Sci. https://doi.org/10.1175/1520-0469(1962)019%3c0244:TSBAAF%3e2.0.CO;2

European Centre for Medium-Range Weather Forecasts (ECMWF) (n.d.) Specific_humidity_from_dewpoint—Metview documentation. Metview. Retrieved August 8, 2024, from https://metview.readthedocs.io/en/latest/api/functions/specific_humidity_from_dewpoint.html

Feng J, Gao K, Santamouris M, Shah KW, Ranzi G (2020) Dynamic impact of climate on the performance of daytime radiative cooling materials. Solar Energy Mater Solar Cells 208:110426. https://doi.org/10.1016/j.solmat.2020.110426

Gershunov A, Guirguis K (2012) California heat waves in the present and future. Geophys Res Lett. https://doi.org/10.1029/2012GL052979
Greene S, Kalkstein LS, Mills DM, Samenow J (2011) An examination of climate change on extreme heat events and climate-mortality relationships in large U.S. cities. Weather Climate Soc. https://doi.org/10.1175/WCAS-D-11-00055.1
Haashemi S, Weng Q, Darvishi A, Alavipanah SK (2016) Seasonal variations of the surface urban heat island in a semi-arid city. Remote Sens 8(4):Article 4. https://doi.org/10.3390/rs8040352
Hanna EG, Tait PW (2015) Limitations to thermoregulation and acclimatization challenge human adaptation to global warming. Int J Environ Res Public Health 12(7):Article 7. https://doi.org/10.3390/ijerph120708034
He C, Kim H, Hashizume M, Lee W, Honda Y, Kim SE, Kinney PL, Schneider A, Zhang Y, Zhu Y, Zhou L, Chen R, Kan H (2022) The effects of night-time warming on mortality burden under future climate change scenarios: a modelling study. Lancet Planet Health 6(8):e648–e657. https://doi.org/10.1016/S2542-5196(22)00139-5
Held I, Soden B (2000) Water vapor feedback and global warming. Ann Rev Energy Environ 25:441–475. https://doi.org/10.1146/annurev.energy.25.1.441
Hossain Md. M., Gu M (2016) Radiative cooling: principles, progress, and potentials. Adv Sci 3(7):1500360. https://doi.org/10.1002/advs.201500360
Hulley GC, Ghent D, Göttsche FM, Guillevic PC, Mildrexler DJ, Coll C (2019) 3—Land surface temperature. In Hulley GC, Ghent D (eds) Taking the temperature of the Earth. Elsevier, pp 57–127. https://doi.org/10.1016/B978-0-12-814458-9.00003-4
Hwang J (2024) Climate-dependent enhancement of radiative cooling with mirror structures. J Photon Energy 14(2):028001. https://doi.org/10.1117/1.JPE.14.028001
Iowa State University (2023) Iowa State University Iowa Environmental Mesonet. ASOS-AWOS-METAR Data Download. Retrieved December 14, 2023, from https://mesonet.agron.iastate.edu/request/download.phtml?network=FL_ASOS
Jiang T, Krayenhoff ES, Martilli A, Nazarian N, Stone B, Voogt JA (2025) Prioritizing urban heat adaptation infrastructure based on multiple outcomes: comfort, health, and energy. Proc Natl Acad Sci U S A 122(19):e2411144122. https://doi.org/10.1073/pnas.2411144122
Kottek M, Grieser J, Beck C, Rudolf B, Rubel F (2006) World map of the Köppen-Geiger climate classification updated. Meteorol Z 15(3):259–263. https://doi.org/10.1127/0941-2948/2006/0130
Läderach A, Raible CC (2013) Lower-tropospheric humidity: climatology, trends and the relation to the ITCZ. Tellus A Dyn Meteorol Oceanogr 65(1):20413. https://doi.org/10.3402/tellusa.v65i0.20413
Lemoine-Rodríguez R, Inostroza L, Zepp H (2022) Intraurban heterogeneity of space-time land surface temperature trends in six climate-diverse cities. Sci Total Environ 804:150037. https://doi.org/10.1016/j.scitotenv.2021.150037
Li M, Peterson HB, Coimbra CFM (2019) Radiative cooling resource maps for the contiguous United States. J Renewable Sustainable Energy 11(3):036501. https://doi.org/10.1063/1.5094510
Litardo J, Del Pero C, Molinaroli L, Leonforte F, Aste N (2022) Sustainable active cooling strategies in hot and humid climates – a review and a practical application in Somalia. Build Environ 221:109338. https://doi.org/10.1016/j.buildenv.2022.109338
Liu C, Wu Y, Wang B, Zhao CY, Bao H (2019) Effect of atmospheric water vapor on radiative cooling performance of different surfaces. Solar Energy 183:218–225. https://doi.org/10.1016/j.solener.2019.03.011
Li X, 'Cathy,' Zhao L, Qin Y, Oleson K, Zhang Y (2024) Elevated urban energy risks due to climate-driven biophysical feedbacks. Nat Clim Change 14(10):1056–1063.https://doi.org/10.1038/s41558-024-02108-w
Manoli G, Fatichi S, Bou-Zeid E, Katul GG (2020) Seasonal hysteresis of surface urban heat islands. Proc Natl Acad Sci U S A 117(13):7082–7089. https://doi.org/10.1073/pnas.1917554117
Masson V, Bonhomme M, Salagnac J-L, Briottet X, Lemonsu A (2014) Solar panels reduce both global warming and urban heat island. Front Environ Sci. https://doi.org/10.3389/fenvs.2014.00014
Matthews T (2018) Humid heat and climate change. Prog Phys Geogr Earth Environ 42(3):391–405. https://doi.org/10.1177/0309133318776490
Mohammed A, Khan A, Saeed Khan H, Santamouris M (2024) On the cooling energy impacts of combined urban heat mitigation strategies in subtropical urban building environment. Energy Build 309:113918. https://doi.org/10.1016/j.enbuild.2024.113918
Murray L, Nguyen H, Lee Y-F, Remmenga M, Smith D (2012) Variance inflation factors in regression models with dummy variables. Conf Appl Stat Agric. https://doi.org/10.4148/2475-7772.1034
Muse N, Clement A, Mach KJ (2024) Daytime land surface temperature and its limits as a proxy for surface air temperature in a subtropical, seasonally wet region. PLoS Climate 3(10):e0000278. https://doi.org/10.1371/journal.pclm.0000278
Muse N, Iwaniec DM, Wyczalkowski C, Mach KJ (2022) Heat exposure and resilience planning in Atlanta, Georgia. Environ Res: Clim 1(1):015004. https://doi.org/10.1088/2752-5295/ac78f9

NASA (n.d.) Temperature over time. Climate Science Investigations. Retrieved July 28, 2024, from https://www.ces.fau.edu/nasa/module-3/why-does-temperature-vary/angle-of-the-sun.php
National Aeronautics and Space Administration (2023) MODIS (Moderate Resolution Imaging Spectroradiometer). About. Retrieved December 14, 2023, from https://mesonet.agron.iastate.edu/request/download.phtml?network=FL_ASOS
National Land Cover Database (2023) Data. Multi-Resolution Land Characteristics Consortium. Retrieved July 7, 2023, from https://www.mrlc.gov/data
National Oceanic and Atmospheric Administration (2023) U.S. Climate Normals. National Centers for Environmental Information (NCEI). Retrieved April 6, 2023, from https://www.ncei.noaa.gov/products/land-based-station/us-climate-normals
National Oceanic and Atmospheric Administration (n.d.) WetBulb Globe Temperature. National Weather Service; NOAA's National Weather Service. Retrieved June 11, 2024, from https://www.weather.gov/tsa/wbgt
National Science Foundation, and MetPy (n.d.) Specific_humidity_from_dewpoint. MetPy v1.6. Retrieved August 8, 2024, from https://unidata.github.io/MetPy/latest/api/generated/metpy.calc.specific_humidity_from_dewpoint.html
National Wildfire Coordinating Group. (n.d.). *7.2 Wet Bulb Temperature*. NWCG. Retrieved June 11, 2024, from https://www.nwcg.gov/course/ffm/atmospheric-moisture/72-wet-bulb-temperature
NOAA and CDC (2024) National Weather Service HeatRisk Prototype. National Weather Service. Retrieved June 24, 2024, from https://www.wpc.ncep.noaa.gov/heatrisk/
NOAA (n.d.-a) Dew Point Statistics for West Central and Southwest Florida. National Weather Service; NOAA's National Weather Service. Retrieved May 18, 2025, from https://www.weather.gov/tbw/dewpoint
NOAA (n.d.-b) *Heat Index Chart*. National Weather Service; NOAA's National Weather Service. Retrieved August 12, 2024, from https://www.weather.gov/ffc/hichart
NV5 Geospatial Software (n.d.). IDL Software. Retrieved June 8, 2025, from https://www.nv5geospatialsoftware.com/Products/IDL
Peng S, Piao S, Ciais P, Friedlingstein P, Ottle C, Bréon F-M, Nan H, Zhou L, Myneni RB (2012) Surface urban heat island across 419 global big cities. Environ Sci Technol 46(2):696–703. https://doi.org/10.1021/es2030438
Petkova EP, Ebi KL, Culp D, Redlener I (2015) Climate change and health on the U.S. Gulf Coast: public health adaptation is needed to address future risks. Int J Environ Res Public Health 12(8):Article 8. https://doi.org/10.3390/ijerph120809342
Pielke RA (1973) A three-dimensional numerical model of the sea breezes over South Florida [Ph.D., The Pennsylvania State University]. Retrieved July 28, 2024, from https://www.proquest.com/docview/302644853/citation/DF939D84EBB4BD7PQ/1
Posit Team (2024) RStudio: integrated development for R (Version 4.3.3) [Posit Software]. PBC. Retrieved July 28, 2024, from http://www.posit.co/
PRISM Climate Group (2023) Time series values for individual locations. Northwest Alliance for Computational Science and Engineering. Retrieved November 9, 2023, from http://www.prism.oregonstate.edu/explorer/
Priyadarsini R, Hien WN, Wai David CK (2008) Microclimatic modeling of the urban thermal environment of Singapore to mitigate urban heat island. Solar Energy 82(8):727–745. https://doi.org/10.1016/j.solener.2008.02.008
Qiu G, Li H, Zhang Q, Chen W, Liang X, Li X (2013) Effects of evapotranspiration on mitigation of urban temperature by vegetation and urban agriculture. J Integr Agric 12(8):1307–1315. https://doi.org/10.1016/S2095-3119(13)60543-2
Raymond C, Matthews T, Horton RM (2020) The emergence of heat and humidity too severe for human tolerance. Sci Adv 6(19):eaaw1838. https://doi.org/10.1126/sciadv.aaw1838
Raymond C, Matthews T, Horton RM, Fischer EM, Fueglistaler S, Ivanovich C, Suarez-Gutierrez L, Zhang Y (2021) On the controlling factors for globally extreme humid heat. Geophys Res Lett 48(23):e2021GL096082. https://doi.org/10.1029/2021GL096082
Roca R, Bergès J-C, Brogniez H, Capderou M, Chambon P, Chomette O, Cloché S, Fiolleau T, Jobard I, Lémond J, Ly M, Picon L, Raberanto P, Szantai A, Viollier M (2010) On the water and energy cycles in the tropics. CR Geosci 342(4):390–402. https://doi.org/10.1016/j.crte.2010.01.003
Rogers CDW, Ting M, Li C, Kornhuber K, Coffel ED, Horton RM, Raymond C, Singh D (2021) Recent increases in exposure to extreme humid-heat events disproportionately affect populated regions. Geophys Res Lett 48(19):e2021GL094183. https://doi.org/10.1029/2021GL094183
Schmitt E, Clement AC (2025) Controls of hyperlocal heat hazard in Miami-Dade County. American Meteorological Society Annual Meeting, New Orleans

Shandas V, Voelkel J, Williams J, Hoffman J (2019) Integrating satellite and ground measurements for predicting locations of extreme urban heat. Climate 7(1):Article 1. https://doi.org/10.3390/cli7010005
Shen L, Zhao C, Ma Z, Li Z, Li J, Wang K (2019) Observed decrease of summer sea-land breeze in Shanghai from 1994 to 2014 and its association with urbanization. Atmos Res 227:198–209. https://doi.org/10.1016/j.atmosres.2019.05.007
Sherwood SC, Dixit V, Salomez C (2018) The global warming potential of near-surface emitted water vapour. Environ Res Lett 13(10):104006. https://doi.org/10.1088/1748-9326/aae018
Sherwood SC, Huber M (2010) An adaptability limit to climate change due to heat stress. Proc Natl Acad Sci U S A 107(21):9552–9555. https://doi.org/10.1073/pnas.0913352107
Stone B Jr., Rodgers MO (2001) Urban form and thermal efficiency. J Am Plan Assoc 67(2):186. https://doi.org/10.1080/01944360108976228
Stull R (2011) Wet-bulb temperature from relative humidity and air temperature. J Appl Meteorol Climatol 50(11):2267–2269. https://doi.org/10.1175/JAMC-D-11-0143.1
Taha H, Akbari H, Rosenfeld A, Huang J (1988) Residential cooling loads and the urban heat island—the effects of albedo. Build Environ 23(4):271–283. https://doi.org/10.1016/0360-1323(88)90033-9
Takebayashi H, Moriyama M (2007) Surface heat budget on green roof and high reflection roof for mitigation of urban heat island. Build Environ 42(8):2971–2979. https://doi.org/10.1016/j.buildenv.2006.06.017
Tomlinson CJ, Chapman L, Thornes JE, Baker C (2011) Remote sensing land surface temperature for meteorology and climatology: a review. Meteorol Appl 18(3):296–306. https://doi.org/10.1002/met.287
Trenberth KE, Dai A, Rasmussen RM, Parsons DB (2003) The changing character of precipitation. Bull Am Meteorol Soc 84(9):1205–1218. https://doi.org/10.1175/BAMS-84-9-1205
Turek-Hankins LL, Cruz M, Brown N, Muse N, Clement A, Mach KJ (2025) Interactions between indoor heat and energy affordability amplify household risks in hot-humid US climate zones. One Earth 8(3):101235. https://doi.org/10.1016/j.oneear.2025.101235
Tysa SK, Ren G, Qin Y, Zhang P, Ren Y, Jia W, Wen K (2019) Urbanization effect in regional temperature series based on a remote sensing classification scheme of stations. J Geophys Res Atmos 124(20):10646–10661. https://doi.org/10.1029/2019JD030948
US Census Bureau (2025) Metropolitan and micropolitan statistical areas population totals: 2020-2024. United States Census Bureau. Retrieved June 24, 2025, from https://www.census.gov/data/tables/time-series/demo/popest/2020s-total-metro-and-micro-statistical-areas.html
US Department of Agriculture (2023) USDA Plant Hardiness Zone Map. 2023 USDA Plant Hardiness Zone Map. Retrieved December 28, 2023, from https://planthardiness.ars.usda.gov/
US EPA, OAR (2024) Climate Change Connections: Florida (The Everglades) [Overviews and Factsheets]. State and Regional Climate Connections. Retrieved June 8, 2025, from https://www.epa.gov/climateimpacts/climate-change-connections-florida-everglades
USGS (2023) EarthExplorer. United States Geological Survey. Retrieved November 10, 2023, from https://earthexplorer.usgs.gov/
Vecellio DJ, Wolf ST, Cottle RM, Kenney WL (2022) Evaluating the 35°C wet-bulb temperature adaptability threshold for young, healthy subjects (PSU HEAT project). J Appl Physiol 132(2):340–345. https://doi.org/10.1152/japplphysiol.00738.2021
Vijayan DS, Sivasuriyan A, Patchamuthu P, jayaseelan R (2022) Thermal performance of energy-efficient buildings for sustainable development. Environ Sci Pollut Res Int 29(34):51130–51142. https://doi.org/10.1007/s11356-021-17602-3
Virmani JI, Weisberg RH (2005) Relative humidity over the West Florida Continental Shelf. Mon Weather Rev. https://doi.org/10.1175/MWR2944.1
Wang X, Li H, Sodoudi S (2022) The effectiveness of cool and green roofs in mitigating urban heat island and improving human thermal comfort. Build Environ 217:109082. https://doi.org/10.1016/j.buildenv.2022.109082
Wan Z, Hook S, Hulley G (2015) MOD11A2 MODIS/Terra land surface temperature/emissivity 8-day L3 global 1km SIN Grid V006. NASA EOSDIS Land Process Distrib Active Arch Center. https://doi.org/10.5067/MODIS/MOD11A2.006
Wickham H (2016) ggplot2: Elegant Graphics for Data Analysis [Computer software]. Springer Verlag. https://ggplot2.tidyverse.org
Winsberg MD (2011) Climate of Florida. Florida Climate Center. https://climatecenter.fsu.edu/images/fcc/climateofflorida.pdf
Wu X, Wang G, Yao R, Wang L, Yu D, Gui X (2019) Investigating surface urban heat islands in South America based on MODIS data from 2003–2016. Remote Sens. https://doi.org/10.3390/rs11101212
Xiao Y, Yang J, Cui L, Deng J, Fu P, Zhu J (2023) Weakened sea-land breeze in a coastal megacity driven by urbanization and ocean warming. Earths Future 11(8):e2022EF003341. https://doi.org/10.1029/2022EF003341

Yang J, Wang Y, Xiao X, Jin C, Xia J (Cecilia), Li X (2019) Spatial differentiation of urban wind and thermal environment in different grid sizes. Urban Clim 28:100458. https://doi.org/10.1016/j.uclim.2019.100458
Yang J, Zhao L, Oleson K (2023) Large humidity effects on urban heat exposure and cooling challenges under climate change. Environ Res Lett 18(4):044024. https://doi.org/10.1088/1748-9326/acc475
Yao R, Luo Q, Li B (2011) A simplified mathematical model for urban microclimate simulation. Build Environ 46(1):253–265. https://doi.org/10.1016/j.buildenv.2010.07.019
Yin X, Yang R, Tan G, Fan S (2020) Terrestrial radiative cooling: using the cold universe as a renewable and sustainable energy source. Science 370(6518):786–791. https://doi.org/10.1126/science.abb0971
Yurchenko E, Volkov A, Kakosyan A (2019) Energy efficient renovation of typical buildings in the subtropics. E3S Web Conf 135:03038. https://doi.org/10.1051/e3sconf/201913503038
Zeng L, Wardlow B, Tadesse T, Shan J, Hayes M, Li D, Xiang D (2015) Estimation of daily air temperature based on MODIS land surface temperature products over the Corn Belt in the US. Remote Sens 7:951–970. https://doi.org/10.3390/rs70100951
Zhang K, Cao C, Chu H, Zhao L, Zhao J, Lee X (2023) Increased heat risk in wet climate induced by urban humid heat. Nature. https://doi.org/10.1038/s41586-023-05911-1
Zhang Y, Dai M (2022) Analysis of the cooling and humidification effect of multi-layered vegetation communities in urban parks and its impact. Atmosphere 13(12):Article 12. https://doi.org/10.3390/atmos13122045
Zhao S, Zhang X (2023) Energy consumption and heat island effect mitigation analysis of different roofs considering superposition coupling. Front Energy Res. https://doi.org/10.3389/fenrg.2022.1047614
Zhou D, Xiao J, Bonafoni S, Berger C, Deilami K, Zhou Y, Frolking S, Yao R, Qiao Z, Sobrino JA (2019) Satellite remote sensing of surface urban heat islands: Progress, challenges, and perspectives. Remote Sens 11(1), Article 1. https://doi.org/10.3390/rs11010048
Zierden DF, Griffin M (2014) Humidity in Florida. Florida State University. Retrieved December 7, 2023, from https://climatecenter.fsu.edu/images/docs/Humidity-in-Florida.pdf
Zonato A, Martilli A, Gutierrez E, Chen F, He C, Barlage M, Zardi D, Giovannini L (2021) Exploring the effects of rooftop mitigation strategies on urban temperatures and energy consumption. J Geophys Res Atmos 126(21):e2021JD035002. https://doi.org/10.1029/2021JD035002

Publisher's Note Springer Nature remains neutral with regard to jurisdictional claims in published maps and institutional affiliations.